Int. J. Heat Mass Transfer. Vol. 29, No. 3, pp. 359–368, 1986
Printed in Great Britain

0017–9310/86 $3.00 + 0.00

Orientation effects on natural convection/radiation heat transfer from pin-fin arrays

E. M. SPARROW and S. B. VEMURI
Department of Mechanical Engineering, University of Minnesota, Minneapolis, MN 55455, U.S.A.

(*Received* 24 *June* 1985 *and in final form* 27 *August* 1985)

Abstract—The heat transfer characteristics of highly populated pin-fin arrays have been investigated for three different orientations in the gravity field: (1) horizontal fins and vertical baseplate, (2) vertical fins and horizontal downfacing baseplate, and (3) vertical fins and horizontal upfacing baseplate. Experiments were performed in air to measure the combined natural convection and radiation heat transfer, and the radiation was determined analytically. Parametric variations were also made of the number of fins and of the baseplate-to-ambient temperature difference. In general, among the three orientations, the vertical upfacing fin array yielded the highest heat transfer rates, followed by the horizontal fin array and the vertical downfacing fin array. With an increase in the number of fins for fixed values of the other parameters, the heat transfer rate increased at first, attained a maximum, and then decreased, thereby defining an optimal fin population. The fractional contributions of radiation to the combined-mode heat transfer were generally in the 25–40% range, with the larger contributions occurring at the smaller baseplate-to-ambient temperature differences. Comparison of the pin-fin results with those for plate fins tends to encourage the use of pin fins.

INTRODUCTION

NATURAL convection is an attractive cooling mechanism for low-power-level devices because, in contrast to forced convection, it avoids the issues of reliability and energy consumption associated with blowers and pumps. To increase the cooling capabilities of natural convection, it is appropriate to augment the transfer surface area by the use of fins. Despite the practical importance of natural-convection-cooled fins, the literature on the subject is remarkably sparse and is confined to a single class of fins, namely, plate fins. Experimental results for plate-finned natural convection systems are presented in [1–6], all of which pertain to air as the cooling medium.

Natural convection in air is generally accompanied by radiation heat transfer. For high-emissivity surfaces, the two modes of heat transfer are of comparable magnitude. Therefore, when such surfaces are employed (e.g. painted, anodized, or otherwise coated metallic surfaces), it is the combined convective/radiative heat transfer that is relevant for design rather than the convective heat transfer alone.

For finned systems that are essentially isothermal (i.e. fin efficiency near unity), the natural convection and radiation are decoupled and are additive. However, for complex geometries, the radiation calculation is difficult and may require the use of approximations which lead to results of uncertain accuracy. When the fins are nonisothermal, the natural convection and radiation are coupled, which compounds the aforementioned geometry-related difficulties. The foregoing discussion underscores the benefits of reporting combined-mode heat transfer results.

The present paper deals with the natural convection/radiation heat transfer characteristics of a class of fins markedly different from those heretofore reported in the literature, namely, circular cylinders (i.e. pin fins) mounted perpendicular to a plane baseplate. Such fins are already in use in applications such as the cooling of electronic equipment, but without open-literature documentation. In practice, the pin fins are deployed in highly populated arrays and are distributed in a regular pattern on the baseplate.

The results to be reported here constitute the second and concluding part of a two-part study of highly populated pin-fin arrays. The study encompassed experiments which yielded the combined-mode (convective/radiative) heat transfer characteristics and an analysis for determining the radiative component of the heat transfer. In the first part of the study [7], attention was directed to systems in which the baseplate is vertical and the fins are horizontal. In practice, however, various orientations of the fin–baseplate assembly may be encountered, depending on the specifics of the application. In the experiments performed in the second part of the study, the orientation of the fin–baseplate assembly was varied parametrically. All told, three orientations were investigated. The first is the aforementioned vertical baseplate/horizontal fin orientation. In the other two, the baseplate is horizontal and the fins are vertical. In one of these, the baseplate and the fins face upward, while in the other, the baseplate and the fins face downward.

In addition to the orientation of the assembly, two other parameters will be varied during the course of the experiments. One of these is the number of fins in the array, the variation of which was aimed at identifying an optimum fin population which maximizes the rate of heat transfer from a given baseplate at a given temperature difference. The other investigated parameter is the baseplate-to-ambient temperature difference, which was varied over the entire practical range

NOMENCLATURE

A_b	surface area of unfinned baseplate	Q	combined-mode heat transfer rate
A_t	total heat transfer surface area	Q_C	natural convection component of Q
D	fin diameter	Q_R	radiation component of Q
g	acceleration of gravity	Ra	Rayleigh number, $[g\beta(T_b - T_\infty)S^3/\nu^2]Pr$
h	combined-mode heat transfer coefficient, $Q/S^2(T_b - T_\infty)$	S	side dimension of baseplate
		T_b	baseplate temperature
k	thermal conductivity	T_∞	ambient temperature.
L	fin length		
N	number of fins	Greek symbols	
Nu	combined-mode Nusselt number, hS/k	β	coefficient of thermal expansion
Pr	Prandtl number	ν	kinematic viscosity.

for applications such as the cooling of electronic equipment. In addition to the main set of experiments, supplementary experiments were performed to examine the response of the heat transfer rate to the size of the wall in which the baseplate is embedded.

The results to be presented include: (1) combined-mode heat transfer rates for all investigated orientations, fin populations, temperature differences and wall configurations; (2) optimum fin populations; (3) radiation fraction of the combined-mode heat transfer; and (4) comparison with plate-fin results.

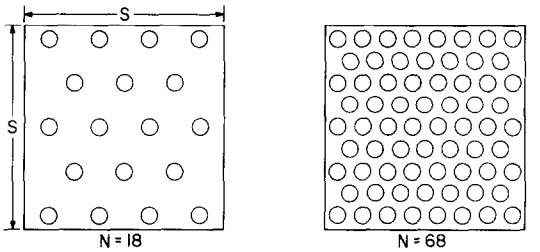

FIG. 1. Head-on views of the fin–baseplate assembly showing the 18-fin and 68-fin arrays.

THE EXPERIMENTS

The description of the experimental apparatus is facilitated by reference to Figs. 1–3. The first of these figures contains two parts, each of which is a head-on view of the baseplate with the fins depicted as circles. The two arrays pictured in Fig. 1 respectively consist of 18 and 68 fins, which correspond to the minimum and maximum fin populations among those investigated. All told, five different arrays were used in the experiments, respectively consisting of 18, 27, 39, 52, and 68 fins. In each of the arrays, the fins were arranged on equilateral-triangular centers, and it is this constraint which is responsible for the seemingly odd numbers of fins (e.g. 39 rather than 40). The baseplate is square with side dimensions S, with $S = 7.62$ cm. Since

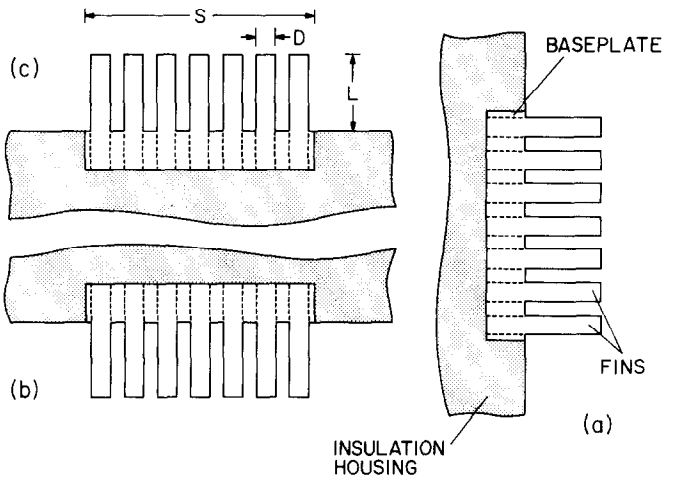

FIG. 2. The three investigated orientations of the fin–baseplate assembly.

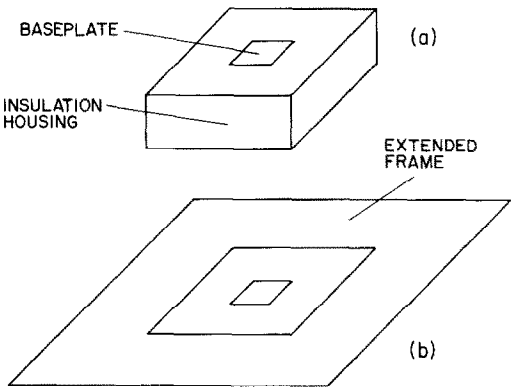

FIG. 3. Insulation housing and extended frame.

the focus of the experiments is to determine the effect of the orientation of the fin–baseplate assembly, the baseplate dimensions, as well as the other geometrical parameters, were held fixed for all the assemblies.

The three investigated orientations of the fin–baseplate assembly are pictured schematically in Fig. 2. In Fig. 2(a), the baseplate is vertical and the fins are horizontal, while Figs. 2(b) and (c) display the horizontal baseplate/vertical fin orientations, respectively downfacing and upfacing. As seen in the figure, the baseplate is inset in an insulation housing such that the exposed surface of the baseplate is flush with the surface of the housing.

The individual fins are rods of diameter $D = 0.635$ cm and exposed length $L = 2.54$ cm. The overall length of each rod is the sum of the exposed length plus the 1.27 cm thickness of the baseplate. To assemble each array, the rods were pressed into appropriately positioned holes drilled through the baseplate. The hole diameter was sized to be 0.0025 cm less than the rod diameter in order to create an interference fit between the rod and the hole. The interference fit served to avoid contact resistance.

Both the fins and the baseplate were made of aluminum. The use of aluminum was based on its high thermal conductivity, its easy machinability, and its receptiveness to a durable, high-emissivity surface coating. The aluminum was black anodized (i.e. coated) after the mating of the fins with the baseplate and after grooves had been milled in the rear face of the baseplate to accommodate electrical resistance wire used for heating the assembly. Closely spaced grooves were used to promote the uniformity of the heating. The emissivity of the anodized aluminum was measured to be 0.82.

The temperature of the baseplate was measured by six embedded thermocouples, which indicated the attainment of virtually isothermal conditions (the deviations were, for the most part, substantially less than $\frac{1}{2}\%$ of the baseplate-to-ambient temperature difference). Thermocouples were also embedded in the tips of 10 strategically located fins. These thermocouples showed that for the 2.54-cm-long fins investigated here, the base-to-tip temperature drop was in the range of 1–2% of the baseplate-to-ambient temperature difference. Therefore, for practical purposes, the fins may be regarded as isothermal (fin efficiency $\cong 1$). For each of the fin–baseplate assemblies and orientations, the baseplate-to-ambient temperature difference was varied from 2 to 70°C.

A pictorial view of the insulation housing with the baseplate in place (but with the fins not shown) is presented in Fig. 3(a). The housing is a rectangular block made from closed-pore polystyrene (Styrofoam) insulation. The face coplanar with the baseplate is a 28×28 cm square, and the thickness is 10.2 cm. To attain hydrodynamic smoothness, the face is covered with white plasticized contact paper (measured emissivity $= 0.855$).

As seen in Fig. 3(a), the insulation housing frames the fin–baseplate assembly (i.e. a 28 cm square which frames a 7.62 cm square). To help quantify the framing effect of the housing, supplementary experiments were performed using the extended frame pictured in Fig. 2(b). The extended frame is believed to be sufficiently large to act as a wall of infinite extent. It is a 61×61 cm square made of stiff cardboard and was mounted to be coplanar with the face of the insulation housing and the baseplate.

Shielded thermocouples situated adjacent to the apparatus measured the ambient temperature. Stratification over a 30-cm height was confined to 0.03°C, and temperature constancy during the course of a 12-h data run was in the same range.

The experiments were performed in an isolated room possessing unique stability and quiescence. The room was never entered during a data run, and the power supply, digital voltmeter and barometer were located in an adjacent room.

Further details of the apparatus and the experimental procedure are available in ref. [8].

DATA REDUCTION AND RADIATION ANALYSIS

The data collected during each run included the electric power input to the fin–baseplate assembly, the baseplate and ambient temperatures, and the barometric pressure. Estimates indicated that heat conduction through the insulation housing was negligible, so that the rate of heat transfer Q from the assembly by convection and radiation was evaluated directly from the power input. As already noted, the baseplate thermocouples yielded virtually uniform readings, and the slight nonuniformities were averaged out in obtaining the baseplate temperature T_b. The occasional 1–2 μV variations in the ambient thermocouple readings were also averaged out in the evaluation of T_∞.

It was desired that both the heat transfer coefficient h and the Nusselt number Nu be direct reflections of the convective/radiative heat transfer rate Q. In particular, changes in h and Nu with fin population and with the

orientation of the assembly should be truly indicative of changes in Q. To this end, h will be based on the surface area $A_b (= S^2)$ of the unfinned baseplate, while the side S of the baseplate will be used as the characteristic length in Nu (note that S is the same for all the assemblies). From these considerations, it follows that

$$h = Q/S^2(T_b - T_\infty) \tag{1}$$

$$Nu = hS/k = Q/Sk(T_b - T_\infty). \tag{2}$$

For a given array population and assembly orientation, the temperature difference $(T_b - T_\infty)$ served as the independent variable of the experiments. The Rayleigh number was chosen as the dimensionless representation of the temperature difference

$$Ra = [g\beta(T_b - T_\infty)S^3/\nu^2]Pr \tag{3}$$

where, again, S is used as the characteristic length. The thermophysical properties appearing in both Ra and Nu were evaluated at a reference temperature equal to $\frac{1}{2}(T_b + T_\infty)$.

As noted in the Introduction, it is the combined convective/radiative heat transfer that is needed in design. The separation of the combined-mode heat transfer into its components can, in principle, be accomplished by analytical–numerical determination of the radiative heat transfer Q_R. In reality, however, the geometry of the investigated fin–baseplate assemblies is so complex as to introduce formidable difficulties into the analysis. Even when reasonable approximations are employed, the analysis is still very difficult and time consuming.

Two key assumptions were used to simplify the radiation analysis. One is that the fins are isothermal at the baseplate temperature T_b. As noted earlier, this assumption is closely approximated by the 2.54-cm-long fins employed here. For the case of the postulated isothermal fin–baseplate assembly, it is convenient to define a new temperature scale

$$\theta^4 = T^4 - T_\infty^4 \tag{4}$$

such that for the assembly $\theta_b^4 = T_b^4 - T_\infty^4$, while for the surroundings $\theta_\infty^4 = T_\infty^4 - T_\infty^4 = 0$. In the new temperature scale, the fins and baseplate radiate at a temperature θ_b^4, but the surroundings are not radiating. This eliminates the need to consider radiation arriving at the assembly from the surroundings.

The second assumption, made to eliminate interreflections among the various exposed surfaces of the assembly, is that the surfaces are black. As noted earlier, the surfaces were black anodized and had a measured emissivity of 0.82. However, the geometry of the assembly defines an array of partially enclosed cavities, and it is well established that the effective emissivity of a cavity can be substantially larger than the actual emissivity of the surfaces which bound the cavity [9, Chap. 6]. From an examination of Fig. 1, it is evident that the more populous the array, the more confined are the cavities and the higher is the effective emissivity. Therefore, the accuracy of the blackbody-based radiation calculation should improve as the number of fins in the array increases. In any event, the assumption of black surfaces tends to somewhat overestimate the radiative component.

The analysis is initiated by imagining a fictive box-like envelope placed over the assembly. The next step is to determine the participating angle factors: (1) from the baseplate to the envelope, (2) from the cylindrical surfaces of the fins to the envelope, and (3) from the tips of the fins to the envelope. This is an extremely difficult task which is described in detail in ref. [8, Chap. 4] and outlined in ref. [7], so that no further exposition is needed here. Approximations were necessary which, if error-producing, tend to underestimate the radiative component.

Although simplifying assumptions were made in the radiation analysis, it is believed that the computed values of the radiation heat transfer are substantially correct. There may be a modest overestimation for the lesser-populated arrays which diminishes as the fin population increases.

RESULTS AND DISCUSSION

Heat transfer

The combined-mode heat transfer results for all of the operating conditions of the experiments are presented in Figs. 4–6. These figures encompass a total of five graphs. Each graph conveys the results for a specific fin–baseplate assembly as characterized by the number of fins N, with $N = 18$ and 27 in Fig. 4, 39 and 52 in Fig. 5, and 68 in Fig. 6. In each graph, there are three sets of data, respectively, for the three orientations. The orientations are keyed to the data symbols in the legend of each figure. In order to achieve conciseness in the legend, only the orientation of the fins is spelled out. The complete description of the orientations is: (1) horizontal fins and vertical baseplate, (2) vertical fins and horizontal baseplate facing downward, and (3) vertical fins and horizontal baseplate facing upward.

The data are plotted in terms of the Nusselt and Rayleigh numbers. However, in view of the specific definitions of these quantities as described in the foregoing, Figs. 4–6 can be regarded as plots of the combined-mode heat transfer rate as a function of the baseplate-to-ambient temperature difference. The open symbols depict data taken without the external frame, while the black symbols represent the supplementary data runs made with the external frame in place. Smooth curves have been passed through the data for continuity.

An overall inspection of Figs. 4–6 indicates that among the three investigated orientations of the fin–baseplate assembly, the highest heat transfer rates were generally attained when the fins were vertical and upfacing. On the other hand, the lowest transfer rates generally occurred for the downfacing vertical fins. The heat transfer attained in the horizontal fin orientation was, globally speaking, bracketed between the values for the two vertical orientations. At the smallest of the

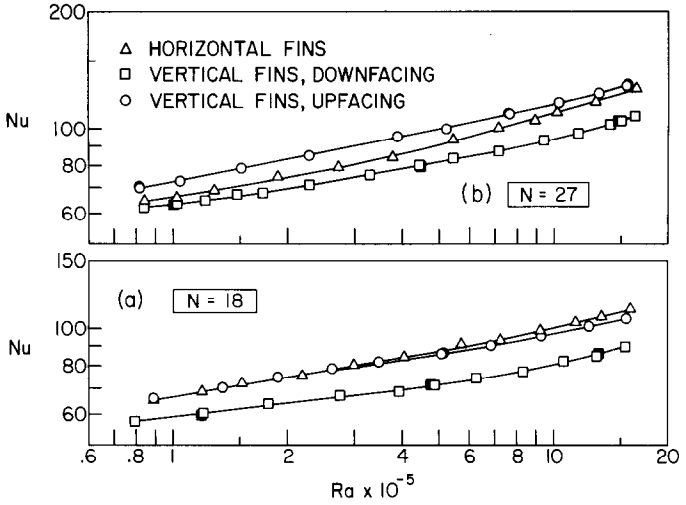

FIG. 4. Nusselt numbers for all three orientations, $N = 18$ and 27.

investigated fin populations [Fig. 4(a)], the heat transfer from the horizontal fin array was essentially equal to (and, at high Ra, slightly surpassed) that from the vertical upfacing fin array. However, as the fin population increased, the *relative* performance of the horizontal array diminished, so that for the most populous case (Fig. 6), its Nu, Ra distribution was more or less coincident with that for the vertical downfacing fin array (and fell slightly below at high Ra).

From the practical standpoint, it is relevant to assess the penalty in heat transfer incurred if design constraints were to mandate the use of the horizontal fin orientation rather than the vertical upfacing fin orientation. Figures 4–6 show that the extent of the penalty depends on the number of fins in the array and on the Rayleigh number (i.e. on the baseplate-to-ambient temperature difference). For the 39-fin array (which, to be documented later, is in the neighborhood of the optimum population) and for $Ra \geqslant 4 \times 10^5$ (the range of practical temperature differences), the heat transfer is 15% smaller when the fins are horizontal than when they are vertical and upfacing. The penalty would be about 20% if downfacing vertical fins were to be used.

The response of the combined-mode heat transfer to the orientation of the fin–baseplate assembly, as evidenced in Figs. 4–6, is due entirely to the response of the natural convection component. This is because the radiative component is independent of orientation (the assembly is essentially isothermal for all the orientations, and the radiative surroundings are unaffected by the orientation). Therefore, it is sufficient to look to the natural convection to rationalize the orientation-related trends in Figs. 4–6.

With regard to the vertical upfacing and vertical

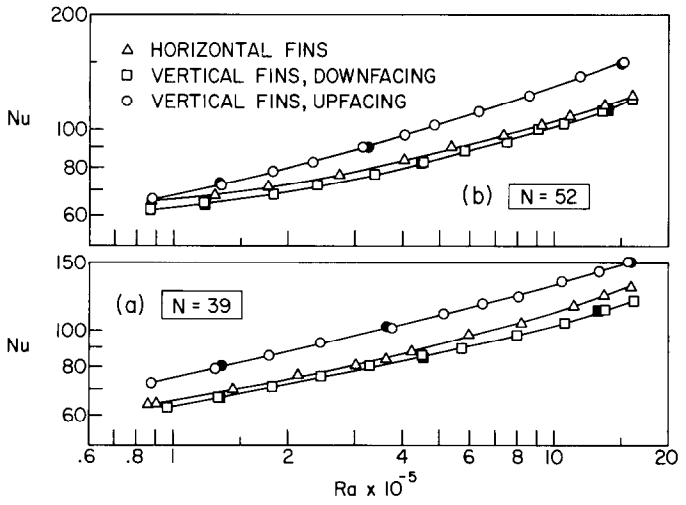

FIG. 5. Nusselt numbers for all three orientations, $N = 39$ and 52.

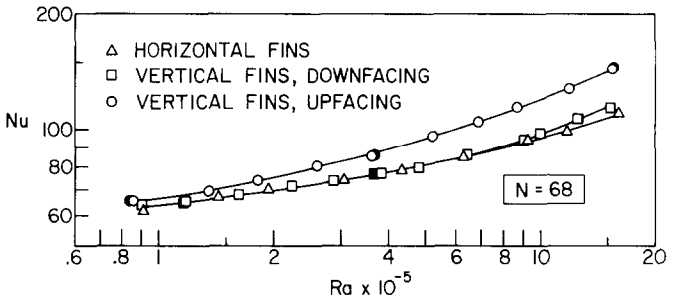

FIG. 6. Nusselt numbers for all three orientations, $N = 68$.

downfacing orientations, it is well established that for the unfinned baseplate, the natural convection is more vigorous for the former than for the latter—a relationship which should, at least, continue to hold for sparsely populated arrays. Furthermore, for the downfacing array, the fin-induced buoyant upflow is stymied due to the blocking action of the baseplate, and the lateral outflow from the array to the surroundings just below the baseplate opposes the inflow of fresh air. These factors work together to give rise to lower rates of transfer for the downfacing orientation.

The *relative* deterioration of the heat transfer performance of the horizontal fin array with increasing fin population is believed due to the increased tendency of the air to thermally saturate in the upper part of the array. This tendency is stronger for the horizontal array because of the longer flow path through the array and because inflow of fresh air can occur at only three of the four sides (the fourth side is blocked by the vertical baseplate).

Attention will now be turned to the effect of the extended frame [Fig. 3(b)] on the Nusselt number results. The data collected with the extended frame in place are depicted by the black symbols in Figs. 4–6. At least three such data runs (low, medium and high Ra) were made for each fin population for both the vertical upfacing and vertical downfacing arrays (in a few instances, the data are totally obscured by overlap).

Inspection of the figures reveals that the black data symbols are in excellent agreement with the open data symbols, indicating no effect of the extended frame. In view of this, the heat transfer results can be regarded as corresponding to a finned heated patch embedded in an extensive surface.

Optimal fin population

The issue now to be addressed is whether, when everything else is held fixed, there is a particular fin population (i.e. an optimal population) which yields a maximum value of the combined-mode heat transfer rate. The existence of such a maximum can be made plausible by considering the variations of the convective and radiative heat transfer rates with increasing fin population. The radiative component increases monotonically with fin population but levels off and approaches an upper bound at large populations. On the other hand, the convective component initially increases and subsequently decreases. The initial increase is due to the increase in transfer surface area with fin population. The subsequent decrease occurs because of the higher resistance to air flow brought about by the tighter interfin clearances which accompany an increase in fin population. Furthermore, the diminished throughflow of air has a greater tendency toward thermal saturation.

With this as background, a graphical presentation will now be made of the variation of the combined-mode heat transfer rate with fin population. Figures 7–9 have been prepared for this purpose, respectively for the horizontal, vertical upfacing, and vertical downfacing fin orientations. In each figure, for each of four Ra values which span the investigated range, the combined-mode Nusselt number is plotted as a function of the number of fins N in the array. The data points appearing in these figures have been read from Figs. 4–6, and smooth curves have passed through the data to provide continuity.

For all Rayleigh numbers which reflect the practical range of baseplate-to-ambient temperature differences (i.e. $Ra \geqslant 4 \times 10^5$), maxima exist. For the horizontal fin array, the maxima occur in the neighborhood of $N = 39$ for all of the investigated Rayleigh numbers. These maxima are, however, rather flat, with the Nusselt number being virtually constant in the range $N = 30$–40. For the vertical fin arrays, the maxima tend to

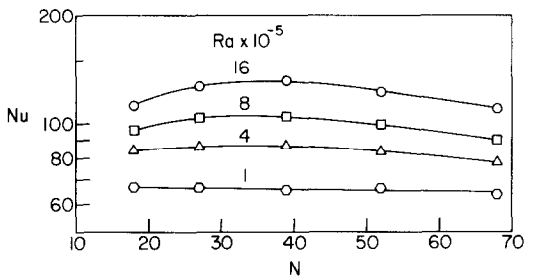

FIG. 7. Dependence of the Nusselt number on the number of fins for the horizontal fin array.

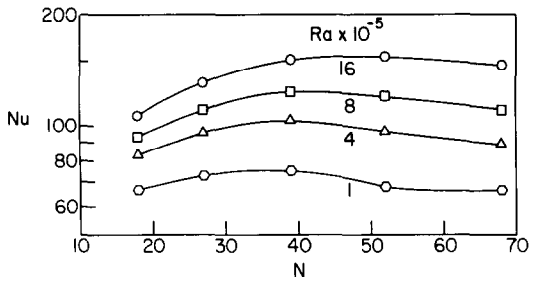

FIG. 8. Dependence of the Nusselt number on the number of fins for the vertical upfacing fin array.

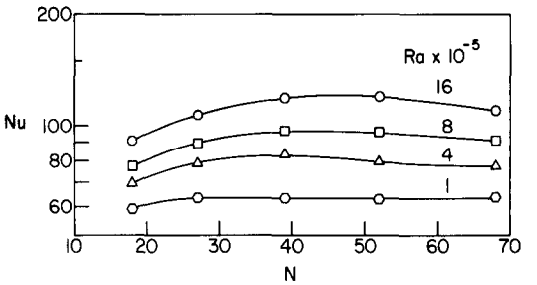

FIG. 9. Dependence of the Nusselt number on the number of fins for the vertical downfacing fin array.

move toward higher N values as the Rayleigh number increases. In particular, the N value at Nu_{max} increases from about 39 to about 50 as Ra increases from 4×10^5 to 16×10^5. Among the three investigated orientations, the Nusselt numbers for the vertical upfacing case display the greatest variation with N.

For the sake of generality, $N \sim 40$ can be regarded as defining the optimum fin population (corresponding to Nu_{max}) for all three fin orientations. The use of this global specification leads to an extreme error of about 2% in identifying Nu_{max}.

Radiation and convection components

Representative results from the radiation heat transfer analysis described earlier in the paper will now be presented. These results will be reported in terms of the Q_R/Q ratio. In this ratio, Q is the experimentally determined, combined-mode heat transfer rate and Q_R is the computed value of the radiative component corresponding to the temperatures T_b and T_∞ of the experiment in which Q was measured. If the convective component is denoted by Q_C, then $Q_C/Q = 1 - Q_R/Q$, so that a presentation of results for Q_R/Q also yields Q_C/Q.

Figure 10 conveys the variation of Q_R/Q with Ra (i.e. with $T_b - T_\infty$) for the case of the horizontal fin orientation and for all the investigated fin populations ($N = 18$–68). Also included for reference purposes is a computed curve which depicts Q_R/Q vs Ra for a vertical flat plate whose dimensions ($S \times S$) are equal to those of the baseplate. The radiation from the plate was computed using an emissivity value of 0.82, which corresponds to that of the anodized aluminum of the present apparatus. The natural convection at the plate surface was evaluated by employing the correlation of ref. [10]. The figure shows that the fractional contribution of radiation to the combined-mode heat transfer is greatest at the smallest temperature difference of the experiments and decreases as the temperature increases. This seemingly unexpected finding can be rationalized by noting that when the temperatures T_b and T_∞ which drive the radiative transfer differ only moderately (compared to their values on the absolute scale), Q_R varies more or less linearly with $(T_b - T_\infty)$. On the other hand, it is well established that natural convection heat transfer varies with the temperature difference to a power greater than one (e.g. 1.25 for many laminar flows). Therefore, the natural convection contribution increases more rapidly with $(T_b - T_\infty)$ than does the radiation component, causing the downsloping trend in Fig. 10.

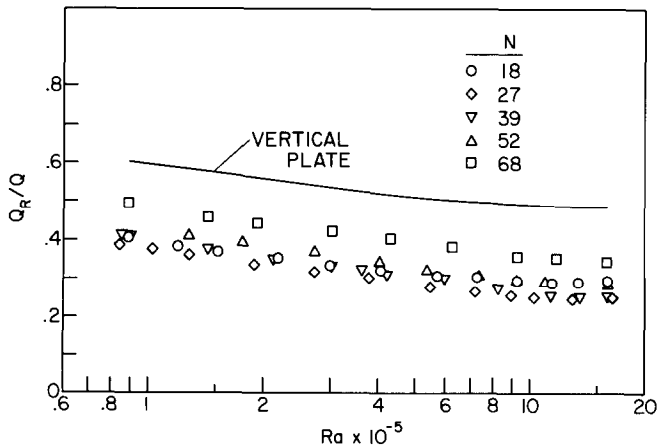

FIG. 10. Fractional contribution of radiation to the combined-mode heat transfer for the horizontal fin array.

At baseplate temperatures greater than those considered here, the nonlinear nature of the radiative transfer will assert itself more and more strongly, so that the Q_R/Q distributions ultimately increase with further increases in the temperature difference.

Most of the Q_R/Q data fall together in a fairly compact band, with only those for the most populous array ($N = 68$) emerging with a clear separate identity. The absence of a strong trend of Q_R/Q with N at small and intermediate N values is believed to be due to the fact that both Q_R and Q_C increase with N in this range. Another factor may be the possible overestimation of the radiation at small N (as discussed earlier) and the decrease of the overestimation as N increases. At larger N, Q_R/Q increases with increasing N, reflecting the dropoff of the natural convection and the continued increase in the radiation.

Aside from the $N = 68$ array, the radiation contribution for the other arrays ranged from 25 to 40% of the combined-mode heat transfer. For the $N = 68$ array, an extreme value of 50% was encountered. It is also interesting to note that the Q_R/Q values for all the fin–baseplate assemblies fall below those for the vertical plate. This suggests that radiation plays a smaller role in the fin heat transfer than it does in the flat plate heat transfer.

The Q_R/Q for the three orientations are brought together in Fig. 11, where the actual data have been omitted in favor of continuous curves in order to preserve clarity. Results are shown for the $N = 27$ and 68 arrays. The $N = 27$ array yielded the lowest Q_R/Q data for the horizontal array (Fig. 10) and virtually the lowest for the other arrays.

Figure 11 shows that the Q_R/Q values for the vertical upfacing array are somewhat reduced relative to those for the horizontal array, indicating the greater effectiveness of convection for the former. On the other hand, for all fin populations except for $N = 68$, the Q_R/Q values for the vertical downfacing array are the greatest among the three orientations, reinforcing the expectation that the convection is least vigorous for that array.

Comparisons with the literature

As noted in the Introduction, there appears to be no information in the literature on either the natural convection or the combined natural convection/radiation heat transfer characteristics of pin-fin arrays. Indeed, the only related configuration for which information is available is that consisting of an array of plate-type fins of rectangular profile attached to a plane baseplate.

It is appropriate to compare the heat transfer performance of pin-fin and plate-fin arrays. A reasonable set of constraints for the comparison might include: (1) equal baseplate dimensions, (2) equal fin length, and (3) equal fin surface area. However, the available information is not sufficient to fulfill these constraints, so that it appears necessary to use a looser set.

To take account of the issue of the baseplate dimensions, the rates of heat transfer per unit unfinned baseplate area A_b will be compared. Note also that the literature for plate fins provides only the natural convection component Q_C, and this requires that Q_C values for the pin fins be used for the comparison (determined by subtracting the computed Q_R from the measured Q). Thus, the quantity that will be compared is $Q_C/A_b(T_b - T_\infty)$. The comparison is made for equal values of fin length ($L = 2.54$ cm) and for area ratios A_t/A_b that are as close as possible to being equal (A_t = total exposed transfer area, A_b = bare baseplate area).

A comparison of plate-fin and pin-fin performance is shown in Fig. 12 for the case in which the baseplate is vertical, where the plate-fin data are from ref. [5, Fig. 1]. The A_t/A_b values for the plotted plate-fin and pin-fin results are 6.62 and 5.54, respectively. The latter (which corresponds to $N = 52$) is the available pin-fin A_t/A_b value which is closest to 6.62.

For the conditions of the comparison, Fig. 12 shows that the pin fins provide better performance than the plate fins (by about 40%). If a comparison similar to Fig. 12 were to be made for the case of the upfacing horizontal baseplate, the outcome would show the pin

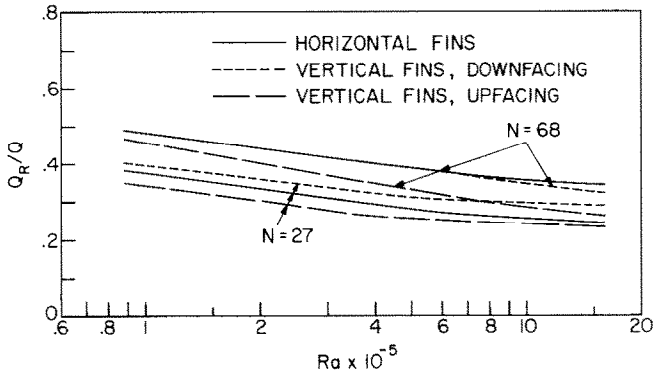

FIG. 11. Fractional contribution of radiation to the combined-mode heat transfer for all three orientations.

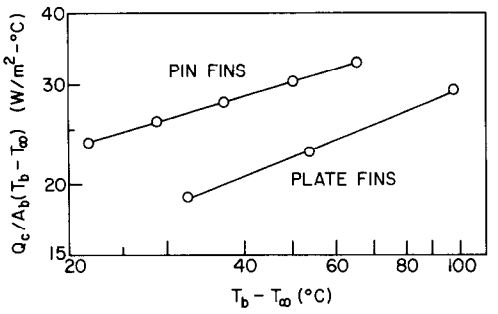

FIG. 12. Comparison of convective heat transfer from plate-fin and pin-fin arrays mounted on vertical baseplates.

fins to be of even greater advantage. Thus, while these comparisons are by no means definitive, they encourage the use of pin fins.

CONCLUDING REMARKS

The research reported here has been concerned with the natural convection/radiation heat transfer characteristics of highly populated pin-fin arrays situated in air. Experiments were performed to measure the combined-mode heat transfer, and the radiation component was determined analytically. The fins were deployed in an equilateral triangular array and mounted perpendicular to a plane baseplate.

The main focus of the research was to determine the response of the combined-mode heat transfer to the orientation of the fin–baseplate assembly in the gravity field. Three orientations were employed: (1) horizontal fins and vertical baseplate, (2) vertical fins and horizontal baseplate facing downward, and (3) vertical fins and horizontal baseplate facing upward. In addition to orientation, parametric variations were made of the number of fins N in the array and of the baseplate-to-ambient temperature difference (i.e. the Rayleigh number Ra).

As the number of fins was increased (while holding all other parameters fixed), the combined-mode heat transfer was found to increase at first, attain a maximum, and then decrease. The N value at the maximum was virtually independent of the Rayleigh number for the horizontal fin array, while for the vertical fin arrays there was a tendency for the maximum to occur at larger N as the Rayleigh number increased. However, with very little loss of accuracy, a common value of N (~ 40 for the present apparatus) can be used to define the optimal fin population for all the investigated orientations and Rayleigh numbers.

In general, among the three orientations, that in which the fins are vertical and the baseplate horizontal and upfacing yielded the highest rates of heat transfer, while the lowest rates were provided by the vertical fin/downfacing baseplate configuration. The heat transfer for the horizontal fin orientation tended to fall between those for the two vertical fin orientations. The actual differences in the heat transfer performance of the three orientations depend on both the fin population and the Rayleigh number. At the aforementioned optimal fin population and for practical values of the Rayleigh number, the heat transfer is about 15% smaller when the fins are horizontal than when they are vertical and upfacing; the heat transfer for the vertical downfacing array is about 20% less than that for the vertical upfacing array.

The fractional contribution of the radiation to the combined-mode heat transfer was found to be greatest at the smallest investigated baseplate-to-ambient temperature difference and diminished as the temperature difference increased. In general, the fractional contribution of the radiation was in the range 25–40%.

Supplementary experiments performed to determine the effect of the face area of the wall in which the baseplate was embedded indicated that the heat transfer results can be regarded as corresponding to a finned, heated patch situated in an extensive surface.

Comparisons of the present pin-fin results with literature information for plate fins tend to encourage the use of pin fins.

REFERENCES

1. K. E. Starner and H. N. McManus, Jr, An experimental investigation of free convection heat transfer from rectangular-fin arrays, *J. Heat Transfer* **85**, 273–278 (1963).
2. J. R. Welling and C. B. Wooldridge, Free convection heat transfer coefficients from rectangular vertical fins, *J. Heat Transfer* **87**, 439–444 (1965).
3. N. Sobel, F. Landis and W. K. Mueller, Natural convection heat transfer in short vertical channels including the effect of stagger, *Proc. 2nd Int. Heat Transfer Conference*, Vol. 2, pp. 121–125 (1966).
4. J. A. Edwards and J. B. Chaddock, An experimental investigation of the radiation and free convection heat transfer from a cylindrical disk extended surface, *Trans. Am. Soc. Heat. Refrig. Air-Condit. Engrs* **69**, 313–322 (1963).
5. J. G. Knudsen and R. B. Pan, Natural convection heat transfer from transverse finned tubes, *Chem. Engng Prog. Symp. Ser.* 61, No. 57, 44–49 (1963).
6. R. R. Laschober and G. R. Sward, Correlation of the heat output of unenclosed single and multiple-tier finned-tube units, *Trans. Am. Soc. Heat. Refrig. Air-Condit. Engrs* **73**, v.3.1–v.3.15 (1967).
7. E. M. Sparrow and S. B. Vemuri, Natural convection/radiation heat transfer from highly populated pin-fin arrays, *J. Heat Transfer* **107**, 190–197 (1985).
8. S. B. Vemuri, Natural convection and radiation heat transfer from highly populated pin-fin arrays. Ph.D. thesis, Department of Mechanical Engineering, University of Minnesota, Minneapolis, MN (1984).
9. E. M. Sparrow and R. D. Cess, *Radiation Heat Transfer*. Hemisphere, Washington (1978).
10. S. W. Churchill and H. H. S. Chu, Correlating equations for laminar and turbulent free convection from a vertical plate, *Int. J. Heat Mass Transfer* **18**, 1323–1329 (1975).

EFFETS D'ORIENTATIONS SUR LE TRANSFERT THERMIQUE CONVECTION NATURELLE/RAYONNEMENT PAR DES ARRANGEMENTS D'AIGUILLES FINES

Résumé—Les caractéristiques thermiques d'arrangements denses d'aiguilles fines sont étudiées pour trois orientations différentes dans le champ de gravité: (1) aiguilles horizontales et plaque-support verticale, (2) aiguilles verticales et plaque-support tournée vers le bas, et (3) aiguilles verticales avec plaque-support tournée vers le haut. Des expériences sont conduites avec l'air pour mesurer la convection naturelle combinée au rayonnement, et le rayonnement est déterminé analytiquement. On fait varier le nombre d'aiguilles et la différence de température entre le support et l'ambiance. En général, parmi les trois orientations, l'arrangement d'aiguilles verticales tournées vers le haut donne les plus forts transferts de chaleur, suivi par (1) puis (2). Quand le nombre d'aiguilles augmente, les autres paramètres étant fixés, le transfert thermique croît d'abord, atteint un maximum, puis décroît, ce qui dégage une population optimale d'aiguilles. Les contributions fractionnelles du rayonnement au transfert global sont de 20 à 40%, avec les plus grandes contributions pour les plus faibles différences de température. La comparaison des résultats avec deux des ailettes planes encourage l'utilisation des aiguilles fines.

EINFLUSS DER ORIENTIERUNG AUF DIE WÄRMEÜBERTRAGUNG DURCH NATÜRLICHE KONVEKTION UND STRAHLUNG VON NADELBERIPPTEN FLÄCHEN

Zusammenfassung—Das Wärmeübertragungsverhalten von sehr dicht mit Nadeln berippten Flächen wurde für drei verschiedene Orientierungen im Schwerefeld untersucht: (1) horizontale Rippen und vertikale Grundplatte, (2) vertikale Rippen und horizontal nach unten gerichtete Grundplatte und (3) vertikale Rippen und horizontal nach oben gerichtete Grundplatte. Die Untersuchungen zur Bestimmung des kombinierten Wärmeübergangs durch natürliche Konvektion und Wärmestrahlung wurden in Luft durchgeführt, wobei der Strahlungsanteil analytisch bestimmt wurde. Als Parameter wurden die Anzahl der Rippen und die Temperaturdifferenz zwischen Grundplatte und Umgebung variiert. Allgemein gilt, daß bei der Anordnung mit den vertikal nach oben gerichteten Rippen das beste Wärmeübertragungsverhalten erreicht wird, gefolgt von den horizontal angeordneten Rippen und der Anordnung mit den vertikal nach unten gerichteten Rippen. Mit zunehmender Anzahl von Rippen—bei konstanten Werten der anderen Parameter—nimmt die Wärmeübertragung zuerst zu, erreicht ein Maximum und nimmt dann ab, womit sich eine optimale Berippungsdichte ergibt. Der anteilige Beitrag der Wärmestrahlung am kombinierten Wärmeübergang war allgemein im Bereich von 25 bis 40%, wobei die größeren Beiträge für kleine Temperaturdifferenzen zwischen Grundplatte und Umgebung erreicht wurden. Der Vergleich der Ergebnisse zwischen mit Nadeln berippten Flächen und solchen mit plattenförmigen Rippen zeigt geringe Vorteile für nadelförmige Rippen.

ЗАВИСИМОСТЬ ЕСТЕСТВЕННОКОНВЕКТИВНОГО И ЛУЧИСТОГО ТЕПЛООБМЕНА ОТ ОРИЕНТАЦИИ РАДИАТОРОВ С ИГОЛЬЧАТЫМИ РЕБРАМИ

Аннотация—Характеристики теплоотдачи от радиаторов с высокой плотностью расположения игольчатых ребер исследовались для трех ориентаций в поле силы тяжести: 1) горизонтальные штыри и вертикальная опорная пластина, 2) вертикальные штыри и горизонтальная опорная пластина, обращенная оребренной стороной вниз, 3) вертикальные штыри и горизонтальная опорная пластина, обращенная оребренной стороной вверх. Эксперименты по измерению комбинированного естественноконвективного и лучистого теплопереноса проводились в воздухе, кроме того, интенсивность излучения определялась аналитически. Варьировались количество штырей и разность температур между опорной пластиной и окружающей средой. Для ориентации с обращенными вверх штырями получены самые высокие коэффициенты теплоотдачи, затем следует радиатор с горизонтальными штырями и, наконец, радиатор с обращенными вниз штырями. С увеличением числа штырей при фиксированных значениях других параметров коэффициент теплоотдачи сначала растет, достигает максимума, а затем уменьшается, что позволяет установить оптимальную плотность штырей. Вклад радиации в комбинированный теплоперенос составлял 25–40%, причем при уменьшении разности температур между опорной пластиной и окружающей средой этот вклад возрастал. Сравнение результатов исследования игольчатых и пластинчатых ребер показало, что предпочтительнее использовать игольчатые.